

Sphingosine-1-phosphate receptor 2 agonist mobilizes endogenous reparative Muse cells that facilitate damaged myocardial tissue repair in rabbit

Shingo Minatoguchi

Gifu University Graduate School of Medicine

Yoshihisa Yamada

Gifu University Graduate School of Medicine

Noriko Endo

Gifu University Graduate School of Medicine

Yoshihiro Kushida

Tohoku University Graduate School of Medicine

Shohei Wakao

Tohoku University Graduate School of Medicine

Hikomitsu Kanamori

Gifu University Graduate School of Medicine

Atsushi Mikami

Gifu University Graduate School of Medicine

Hiroyuki Okura

Gifu University Graduate School of Medicine

Mari Dezawa

Tohoku University Graduate School of Medicine

Shinya Minatoguchi (✉ minatos@gifu-u.ac.jp)

Gifu Municipal Hospital

Article

Keywords: endogenous Muse cells, sphingosine-1-phosphate receptor 2 agonist, mobilization, myocardial infarction, cardiac function, infarct size

Posted Date: May 9th, 2022

DOI: <https://doi.org/10.21203/rs.3.rs-1606323/v1>

License:  This work is licensed under a Creative Commons Attribution 4.0 International License.

[Read Full License](#)

Abstract

Muse cells, SSEA-3(+) non-tumorigenic pluripotent stem cells, reside in the bone marrow (BM), peripheral blood and organ connective tissue as cells. Circulating Muse cells, either endogenous or exogenously administered, selectively accumulate to damaged tissue by sensing sphingosine-1-phosphate (S1P) produced by the damaged tissue, differentiate into tissue-constituent cells including vascular cells, replace apoptotic/damaged cells and repair the tissue. They are expandable to clinical scale and are applied to clinical trials. Acute myocardial infarction model (AMI) model rabbits were subcutaneously injected either with vehicle, S1PR2-agonist, or S1PR2-agonist + S1PR2-antagonist. The S1PR2-agonist group showed the statistically meaningful increase of the endogenous peripheral blood-Muse cell number at 12 h (both $p < 0.05$), reduction of the infarct size ($p < 0.05$) and improvement of the left ventricular function ($p < 0.05$) at 2 weeks compared with the other 2 groups. The increase in peripheral blood-Muse cells positively correlated with LV ejection fraction, and inversely correlated with infarct size in statistical analysis. Green fluorescent protein (GFP)-autologous BM-Muse cells were transplanted back into the BM of the same animal, AMI model was made 48 hrs after, and then vehicle or S1PR2 agonist was administered subcutaneously. At 2 weeks, the number of GFP-Muse cells positive for cardiac markers, troponin-I, α -actinin and connexin-43, and those positive for vascular marker CD31, was higher in the border areas in the S1PR2-agonist group compared with that in the vehicle group. Along with administration of exogenous stem cells, the efficient mobilization of endogenous stem cells such as S1PR2-agonist for Muse cells, might be an alternative promising therapeutic approach.

1. Introduction

Acute myocardial infarction (AMI), particularly large and transmural infarctions, alters both infarcted and non-infarcted regions of the left ventricle (LV), resulting in a thinner LV wall and greater LV dilation, termed LV remodeling, and leading to a deterioration of LV function and a poor prognosis for survival.¹ Despite extensive efforts to prevent AMI and improve outcomes, AMI remains a leading causes of morbidity and mortality worldwide.^{2,3} Even when coronary reperfusion is successful, deterioration of the LV ejection fraction (LVEF) and LV remodeling occur after AMI and these factors predict the long-term prognosis; higher recovery of the LVEF and smaller LV dilation are associated with a better long-term prognosis and the converse is also true.^{4,5} Therefore, fundamental treatment following AMI is critically required to repair the infarcted myocardial tissues, improve the LV function, attenuate LV dilation, and improve the prognosis.

Multilineage-differentiating stress-enduring (Muse) cells are non-tumorigenic endogenous pluripotent-like stem cells identified as pluripotent surface marker stage-specific embryonic antigen-3 positive (SSEA-3+) cells in the bone marrow (BM; corresponding to $\sim 0.03\%$ of the mononucleated fraction), peripheral blood ($\sim 0.04\%$ of mononucleated cells), and connective tissue of various organs.⁶⁻¹⁰ Muse cells are unique because: 1) the number of endogenous Muse cells in the peripheral blood, possibly mobilized from the BM, rapidly increases after tissue damage as shown by stroke and myocardial infarction patients^{8,11}, as

well as after cardiac rehabilitation which improves prognosis of AMI¹² and 2) intravenously administered exogenous Muse cells selectively home to the damaged tissue and replace damaged/apoptotic cells by spontaneous differentiation into the corresponding cell types that comprise the tissue including vascular cells and repair the tissue.¹³⁻¹⁸ We recently reported that AMI patients with higher mobilization of endogenous peripheral blood-Muse cells in the acute phase exhibited statistically meaningful improvement of LV function and attenuation of LV remodeling in the chronic phase at 6 months after onset when compared with patients who exhibited no such increase in the acute phase.⁸ This observation suggested that the number of endogenous peripheral blood-Muse cells correlates with one's reparative activity. In animal models of AMI,¹³ stroke, epidermolysis bullosa, chronic kidney disease, liver cirrhosis, and corneal scarring,^{10, 14-17} intravenous administration of exogenous Muse cells leads to efficient tissue repair and functional recovery. In a rabbit AMI model, we recently reported that selective homing of intravenously infused exogenous Muse cells into the infarcted myocardium was mediated via the sphingosine-1-phosphate (S1P)-S1P receptor 2 (S1PR2) axis –an interaction between S1P produced by the damaged heart and S1PR2 expressed in Muse cells.¹³ After selective homing, Muse cells spontaneously differentiated into physiologically functional cardiomyocytes as well as into blood vessels in the post-infarct tissue, resulted in a significant reduction of infarct size, improvement of LV function, and attenuation of LV remodeling.¹³ Moreover, allogeneic-Muse cells were able to escape from host immunorejection after intravenous administration and survived in the host tissue as differentiated cells for over 6 months, even without immunosuppressive treatment, which is partly explained by the expression of human leukocyte antigen (HLA)-G, which mediates immune tolerance in the placenta.¹³ Furthermore, Muse cells are contained as several percent in mesenchymal stem cells (MSCs) and fibroblasts, and are expandable to clinical scale because they proliferate at the speed comparable to that of fibroblasts.⁶⁻¹⁰ On the basis of these unique properties, intravenously administered donor-derived Muse cells have been applied to clinical trials for the treatment of AMI,¹⁹ stroke, spinal cord injury, epidermolysis bullosa,²⁰ neonatal hypoxic ischemic encephalopathy, amyotrophic lateral sclerosis and acute respiratory distress syndrome associated with SARS-CoV-2 infection under approval of regulatory authorities, all without HLA matching test or long-term immunosuppressant treatment.

We considered that inducing the efficient mobilization of 'endogenous-Muse cells' from the BM into the peripheral circulating blood may promote homing of Muse cells to the damaged post-infarct tissue and deliver tissue repair, similar to the treatment with exogenous Muse cell administration. Activation of endogenous Muse cells might create less of a burden on the patient and improve patient treatment costs. In addition, activation of endogenous Muse cells is more accessible than using expanded autologous cultured Muse cells and/or donor-derived Muse cells. While S1P is a candidate molecule for inducing the mobilization of endogenous Muse cells, it could also evoke the mobilization of inflammatory cells through S1PR1.²¹ We therefore hypothesized that an S1PR2 agonist, rather than S1P, could be an efficient selective mobilizer of endogenous Muse cells. The purpose of this study was to investigate whether post-infarct treatment with an S1PR2 agonist SID46371153²² efficiently mobilizes endogenous Muse cells into the peripheral blood, and whether the mobilized Muse cells engraft into the post-infarct tissue,

differentiate into cardiac and vessel cells, and deliver statistically meaningful tissue repair and functional recovery in a rabbit model of AMI.

2. Materials And Methods

In this study, all rabbits received humane care and the experiments were carried out in strict accordance with the recommendations of the Standards Relating to the Care and Management of Laboratory Animals and Relief of Pain (2006) published by the Japanese Ministry of the Environment, and with the Guide for the Care and Use of Laboratory Animals, published by the US National Institutes of Health (NIH Publication, 8th Edition, 2011). The study protocol was approved by the Committee for Animal Research and Welfare of Gifu University, Gifu, Japan (Permit Number: 25-10). The experiment was performed according to the ARRIVE Guidelines (<https://www.nc3rs.org.uk/arrive-guidelines>).

2.1 Rabbit AMI model

Healthy male Japanese white rabbits (weighing approximately 2.0–2.5 kg) were used. We used only male rabbits to avoid confounding hormonal effects. The investigators who evaluated the outcomes were blinded to the treatment protocols, and the AMI rabbits were randomly assigned to groups using sealed envelopes for the experiments.

The surgical procedure was performed following to the previously reported methods.^{13, 23, 24} Briefly, the rabbits were anesthetized by an intravenous injection of ketamine (10 mg/kg, Ketalar 200mg/20mL, DAIICHI SANKYO COMPANY, LIMITED, Tokyo, JAPAN) and xylazine (3 mg/kg, Selactar 2%, Bayer Yakuhin Ltd., Osaka, JAPAN) via ear veins, and additional doses (half dose of each) were given when required throughout the surgery via a jugular vein according to the guidelines of LABIO 21 (<http://www.nichidokyo.or.jp/>) and ARRIVE Guidelines (<https://www.nc3rs.org.uk/arrive-guidelines>). Once anesthetized, the animals were intubated and ventilated with room air supplemented with a low flow of oxygen using a mechanical ventilator (tidal volume: 25–35 mL, respiratory rate: 20–30/min; Shimano, model SN-480-5, Tokyo, Japan). Serial blood gas analysis was performed, and ventilatory conditions were adjusted to maintain the arterial blood gas within the physiologic range. Surgery was performed under sterile conditions. The carotid artery and jugular veins were cannulated to monitor peripheral arterial pressure and to administer the drugs, respectively. Thereafter, the rabbits were systemically heparinized (500 U/kg), a thoracotomy was performed in the left fourth intercostal space, and the heart was exposed after excising the pericardium. A 4-0 silk suture on a small curved needle was passed through the myocardium beneath the middle segment of the large arterial branch coursing down the middle segment of the anterolateral surface of the left ventricle. Both ends of the silk suture were then passed through a small vinyl tube, and the coronary branch was occluded by pulling the snare, which was fixed by clamping the tube with a mosquito hemostat. Myocardial ischemia was induced for 30 min. Myocardial ischemia was confirmed by ST-segment elevation on electrocardiogram and regional cyanosis of the myocardial surface. Reperfusion was confirmed by myocardial blush over the risk area and a decrease in the ST elevation after releasing the snare. Sham operated animals were prepared using

the same surgical procedures as described for the AMI animals except that the arterial branch was not occluded.

2.12 Statistical analysis

All values are presented as the mean \pm standard error (SE). The normality of the data distributions was tested using the Kolmogorov-Smirnov test. The significance of differences between 2 groups for normally distributed variables was determined by the unpaired Student's t-test. The significance of differences among more than 3 groups for normally distributed variables was evaluated by 1-way analysis of variance followed by multiple comparisons with the Tukey or Dunnett method. Correlation coefficients between 2 variables were obtained by linear regression analysis. All statistical analyses were performed using GraphPad Prism 7 (GraphPad Software Inc.). Values of $p < 0.05$ (*) were considered significant, and values of $p < 0.01$ (**) and $p < 0.001$ (***) were considered highly significant.

Additional Materials and Methods are provided in the Online Data Supplement.

3. Results

3.1 Effect of S1PR2 agonist and antagonist on rabbit Muse cell migration in vitro

In the in vitro migration assay using matrigel invasion chamber, a significantly greater number of rabbit BM-Muse cells actively migrated to the rabbit AMI serum compared with the normal intact rabbit serum ($p < 0.001$; *Figure 1A*). In addition, Muse cells migrated toward the S1PR2 agonist SID46371153 in a concentration-dependent manner (*Figure 1B*). On the other hand, the S1PR2 antagonist JTE-013 efficiently suppressed the migration of Muse cells toward the AMI serum in a concentration-dependent manner (*Figure 1C*). These findings indicated that the S1PR2 agonist and antagonist controlled the migration of rabbit peripheral blood-Muse cells.

3.2 Isolation of rabbit peripheral blood-Muse cells

On the basis of flow cytometric analysis, human Muse cells are contained mainly in the mononuclear cell fraction of the peripheral blood⁸; therefore, we gated the mononuclear area comprising the monocyte and lymphocyte fractions in the rabbit peripheral blood. Scattergrams of unstained cells (*Figure 1D*), SSEA-3⁺ cells (*Figure 1E*), and SSEA-3⁺/CD44⁺ cells (*Figure 1F*) in the mononuclear area of the sham group demonstrated staining specificity in the fluorescence-minus-one control method.

3.3 Mobilization of Muse cells into the peripheral blood was promoted by an S1PR2 agonist

AMI rabbits received a subcutaneous injection of DMSO (vehicle group) or 10 mg/kg of S1PR2 agonist SID46371153 (S1PR2 agonist group) at 30 min after coronary reperfusion, and the peripheral blood was analyzed by flow cytometry 12 h after AMI.

Typical flow cytometry results of the peripheral blood-mononuclear cell fraction in the vehicle and S1PR2 agonist groups are shown in *Figure 2A* and *2B*, respectively. Consistent with a previous report,¹³ SSEA-3⁺ (pluripotent surface marker)/CD44⁺ (mesenchymal marker confirmed to be active in rabbit) cells, corresponding to rabbit Muse cells, were detected using the first gate. The distribution of Muse cells in the monocyte and lymphocyte areas within the gated area was then determined by the previously described method.⁸ The results demonstrated that Muse cells were mainly included in the monocyte area and fewer Muse cells were included in the lymphocyte area in both the vehicle and S1PR2 agonist groups; in the vehicle group, ~43.1% of Muse cells were in the monocyte area and ~7.6% were in the lymphocyte area, and in the S1PR2 agonist group, ~60.8% in the monocyte area and ~12.4% in the lymphocyte area (*Figure 2A,B*). Therefore, Muse cell measurement was performed by focusing on the monocyte region.

The number of SSEA-3⁺/CD44⁺-Muse cells in the peripheral blood was the greatest in the S1PR2 agonist group ($174 \pm 14/100 \mu\text{L}$) compared with the sham ($p < 0.0001$), vehicle ($p < 0.05$), and S1PR2 agonist +antagonist (JTE013) ($p < 0.05$) groups at 12 h after AMI (*Figure 2C*). A higher number of Muse cells was detected in the vehicle group ($130 \pm 7/100 \mu\text{L}$) compared with the sham group ($75 \pm 3/100 \mu\text{L}$, $p < 0.05$; *Figure 2C*). The increase of Muse cell number was abolished by co-injection of JTE013 in the S1PR2 agonist+antagonist group ($122 \pm 20 /100 \mu\text{L}$), with the Muse cell number in the peripheral blood similar to that in the vehicle group (*Figure 2C*). The number of SSEA-3⁺/CD44⁺-Muse cells detected in the S1PR2 agonist group was significantly higher than that detected in the S1PR2 agonist+antagonist groups ($p < 0.05$; *Figure 2C*). Subcutaneously administered SID46371153 was confirmed to be transferred to the blood by measuring the plasma level of SID46371153 in all 4 groups; similar levels of SID46371153 were detected in the S1PR2 agonist and S1PR2 agonist+antagonist groups at 12 h after AMI, but not in the sham and vehicle groups (*Figure S1*).

The number of whole cells in the lymphocyte area (*Figure 2D*) and in the monocyte area (*Figure 2E*) did not differ significantly among the sham, vehicle, and S1PR2 agonist groups, suggesting that the S1PR2 agonist did not evoke the mobilization of immune cells into the peripheral blood at 12 h after administration.

3.4 Physiologic findings

We evaluated the cardiac function in rabbits receiving vehicle, S1PR2 agonist, and S1PR2 agonist+antagonist at 2 weeks after AMI. No differences in the heart rate or systolic and diastolic blood pressures were detected among the vehicle, SID46371153, and JTE013 groups (data not shown). In echocardiography and cardiac catheterization studies, however, the LVEF, LVFS, +dP/dt, and -dP/dt values were significantly higher in the S1PR2 agonist group compared with the vehicle and S1PR2 agonist+antagonist groups (LVEF: $p < 0.001$ compared both with the vehicle and S1PR2 agonist+antagonist groups [*Figure 3A*], LVFS: $p < 0.001$ compared both with the vehicle and S1PR2 agonist+antagonist groups [*Figure 3B*], +dP/dt: $p < 0.001$ compared both with the vehicle and S1PR2 agonist+antagonist groups [*Figure 3C*], and -dP/dt: $p < 0.05$ compared both with the vehicle and S1PR2 agonist+antagonist groups [*Figure 3D*], and the LVDd and LVDs values were significantly lower (LVDd:

$p < 0.001$ compared with the vehicle group and $p < 0.05$ compared with the S1PR2 agonist+antagonist group [Figure 3E] and LVDs: $p < 0.001$ compared with the vehicle group and $p < 0.01$ compared with the S1PR2 agonist+antagonist group [Figure 3F]). The number of Muse cells in the peripheral blood positively correlated with the LVEF value ($p < 0.05$) (Figure 3G).

3.5 Myocardial infarct size

Figure 4A shows plasma troponin T levels 24 h after AMI. Plasma troponin T levels which closely correlate with infarct size²⁵, were substantially increased at 24 h after AMI in all three groups with no significant differences among the groups, suggesting equivalent infarction induction before the administration of S1PR2 agonist.

Figure 4B shows typical examples of a transverse LV section at the papillary muscle level stained by Masson-trichrome at 2 weeks after AMI. The infarct size shown as the percent of the total LV area was significantly smaller in the S1PR2 agonist group ($18.4 \pm 1.8\%$) than in the vehicle group ($26.5 \pm 1.8\%$, $p < 0.05$; Figure 4C). The reduction of the infarct size by the S1PR2 agonist was abolished by the presence of JTE013 (S1PR2 agonist + antagonist group; $26.4 \pm 4.1\%$, $p < 0.05$; Figure 4C). The number of Muse cells in the peripheral blood inversely correlated with the infarct size ($p < 0.05$; Figure 4D).

3.6 Effect of the S1PR2 agonist on cardiomyocyte apoptosis

On day 3 after AMI, TUNEL-positive myocytes were observed in the peri-infarct areas, and the number of TUNEL-positive cardiomyocytes was significantly reduced in the S1PR2 agonist group ($7.9 \pm 0.5\%$) compared with the vehicle group ($16.5 \pm 1.0\%$, $p < 0.001$; Figure 4E).

3.7 Effect of the S1PR2 agonist on CD31-positive microvessels

At 2 weeks after AMI, CD31⁺ (vascular endothelial cell marker) vessels were observed in the peri-infarct areas. The density of the CD31⁺ microvessels (capillary density), counted according to the previous report¹³, was greater in the infarct border area of the S1PR2 agonist group ($1081 \pm 98/\text{mm}^2$) than in the control group ($486 \pm 76/\text{mm}^2$, $p < 0.01$; Figure 4F).

3.8 Differentiation marker expression in engrafted Muse cells

To trace the engraftment of Muse cells mobilized by the S1PR2 agonist into the post-infarct heart, rabbits underwent transplantation of autologous GFP-labeled Muse cells back into the BM of the same animal, the tissue considered to reserve endogenous Muse cells,⁸ and then S1PR2 agonist was injected 30 min after AMI.

Two weeks later, GFP-Muse cells were detected in the infarct border area of the myocardium and the number of integrated Muse cells was significantly greater in the S1PR2 agonist group than in the vehicle group ($p < 0.05$; Figure 5A, 5B). Engrafted GFP-Muse cells expressed cardiac troponin-I and sarcomeric α -actinin in the infarct border area both in the S1PR2 agonist (Figure 5C, 5D) and vehicle groups (Figure 5E,

5F). Connexin43 was detected between the host cardiomyocyte and GFP⁺ Muse cells in the S1PR2 agonist group (*Figure 5G*). The number of GFP⁺/cardiac troponin⁺ cells was significantly greater in the S1PR2 agonist group (8.5 ± 0.7 cells/mm²) than in the vehicle group (2.4 ± 0.3 cells/mm², $p<0.05$; *Figure 5H*). The number of GFP⁺/α-actinin⁺ cells was significantly greater in the S1PR2 agonist group (6.4 ± 0.4 /mm²) than in the control group (1.8 ± 0.0 /mm², $p<0.05$; *Figure 5H*).

GFP-Muse cells were also incorporated into vessels as CD31⁺ cells in the S1PR2 agonist and vehicle groups (*Figure 5I, 5J*). The number of GFP and CD31 double-positive cells was significantly greater in the S1PR2 agonist group (16.5 ± 2.1 /mm²) than in the vehicle group (9.0 ± 2.0 /mm², $p<0.05$; *Figure 5K*).

4. Discussion

The present study demonstrated that post-infarct treatment with an S1PR2 agonist compared with vehicle in a rabbit model of AMI significantly: 1) increased mobilization of endogenous SSEA-3⁺/CD44⁺-rabbit Muse cells in the peripheral blood; 2) increased the number of engrafted Muse cells in the infarct border area; 3) reduced the myocardial infarct size, improved LV function, and attenuated LV remodeling, partly due to the differentiation of Muse cells into troponin I⁺, α-actinin⁺, and connexin43⁺ cardiac-lineage cells as well as into CD31⁺ vascular cells; 4) reduced the number of TUNEL-positive cardiomyocytes in the peri-infarct areas; and 5) increased the vascular density at the infarct border area.

We previously reported that AMI patients with higher mobilization of endogenous peripheral blood-Muse cells in the acute phase correlated with an improvement of LV function and attenuation of LV remodeling in the chronic phase at 6 months after AMI as compared with patients who exhibited no such increase in the acute phase.⁸ This suggests that an S1PR2 agonist such as SID46371153 which mobilized endogenous Muse cells in the present study may play an important role in improving LV function and attenuating LV remodeling in the chronic phase.

The number of SSEA-3⁺/CD44⁺-Muse cells in the peripheral blood increased after AMI (vehicle group) compared with the baseline level (sham group), suggesting that AMI itself leads to the mobilization of endogenous Muse cells into the peripheral blood. This finding is consistent with our previous report that endogenous Muse cells are mobilized into the peripheral blood in patients with AMI in the acute phase.⁸

Subcutaneously administered SID46371153 (S1PR2 agonist) was confirmed to be transferred to the blood (*Figure S1*). The number of peripheral blood-Muse cells increased further when the S1PR2 agonist was administered subcutaneously (S1PR2 agonist group), an effect that was counteracted by prior administration of the S1PR2-specific antagonist JTE-013 (S1PR2 agonist + antagonist group; *Fig. 2C*), suggesting that the S1PR2 agonist enhanced the mobilization of Muse cells into the peripheral blood. We previously reported that human Muse cells that predominantly express S1PR2 among all the S1PR subtypes preferentially migrate to the post-infarct border area where the S1P level is highest.¹³ We also reported that rabbit-BM-Muse cells actively migrate to the S1PR2 agonist SID46371153 in an in vitro

study.¹³ In the present study, we newly demonstrated *in vitro* that rabbit-Muse cells migrated to the serum obtained from a rabbit AMI model (Fig. 1A) and an S1PR2 agonist (Fig. 1B), but that the migration was suppressed by the S1PR2 antagonist JTE-013 in a concentration-dependent manner (Fig. 1C). These *in vitro* studies indicate that the S1PR2 agonist and antagonist efficiently controlled the increase and decrease, respectively, in the number of endogenous peripheral blood-Muse cells in the rabbit AMI model (Fig. 2C).

We also investigated whether the S1PR2 agonist affected the total cell number in the lymphocyte area and monocyte area. We found no significant difference in the total cell number in the sham, vehicle, and S1PR2 agonist groups, suggesting that the S1PR2 agonist did not evoke the mobilization of immune cells such as lymphocytes and monocytes (Fig. 2D,2E). Thus, these findings suggest that the cardiac function recovery, the smaller infarct size, lower number of apoptotic cardiomyocytes, higher vessel concentration, and higher marker expression of cardiac and vascular lineages of engrafted Muse cells were due to the increased number of endogenous peripheral blood-Muse cells and not to an increase of immune cells.

With regard to cardiac function and remodeling, administration of the S1PR2 agonist significantly increased LVEF, LVFS, +dP/dt, and -dP/dt (Fig. 3A-3D), and significantly decreased LVDD and LVDs (Fig. 3E,3F) as compared with the vehicle group, suggesting the improvement of LV function and attenuation of LV remodeling. The improvement in the LV function and attenuation of LV remodeling were almost completely reversed by treatment with the S1PR2 antagonist JTE-013 (Fig. 3A-3F). The number of Muse cells in the peripheral blood after AMI positively correlated with the LVEF (Fig. 3G), suggesting that a higher number of Muse cells in the peripheral blood is associated with improved LV function.

The infarct size was significantly reduced in the S1PR2 agonist group compared with the vehicle group at 14 days after AMI (Fig. 4B, 4C). This effect was completely abolished by treatment with the S1PR2 antagonist JTE-013 (Fig. 4B, 4C). The number of Muse cells in the peripheral blood inversely correlated with the infarct size (Fig. 4D), suggesting that a higher number of Muse cells in the peripheral blood is associated with a reduced infarct size.

In the present study, we hypothesized that Muse cells in the peripheral blood could be mobilized from the BM by treatment with an S1PR2 agonist. To define whether AMI itself and an S1PR2 agonist mobilize Muse cells from the BM into the peripheral blood and engraft Muse cells to the damaged heart, autologous BM-Muse cells labeled with GFP were transplanted back into the BM of the iliac crest 48 h prior to AMI induction, and then vehicle or S1PR2 agonist SID46371153 was administered subcutaneously at 30 min after the onset. At 2 weeks after AMI, confocal microscopy demonstrated that GFP-positive Muse cells were detected mainly in the infarct border area (Fig. 5A), and the number of GFP-Muse cells was significantly greater in the S1PR2 agonist group than in the vehicle group (Fig. 5A, 5B). Consistent with our previous report¹³, the engrafted Muse cells expressed cardiac troponin I and sarcomeric α -actinin, suggesting that the Muse cells differentiated into cardiac-lineage cells (Fig. 5C-5F). The presence of a gap junction between host-cardiomyocytes and GFP-Muse cells was suggested by the

expression of connexin43 (Fig. 5G). The engrafted GFP-Muse cells expressed CD31, a marker of vascular endothelial cells, in the infarct border area, suggesting differentiation into vascular cells (Fig. 5I, 5J). Furthermore, the numbers of troponin I⁺/GFP⁺, actinin⁺/GFP⁺, and CD31⁺/GFP⁺ cells were significantly greater in the S1PR2 agonist group than in the vehicle group (Fig. 5H, 5K). The precise number of mobilized Muse cells from the BM of the whole body was not determined due to methodologic limitations. Together, these findings suggest that the infarct size-reducing effect of the S1PR2 agonist was related to the increase in the number of peripheral blood-endogenous Muse cells.

We previously reported that intravenously administered exogenous Muse cells successfully reduced infarct size by multiple actions, including replacing cardiomyocytes and vessels by differentiation of Muse cells and paracrine effects delivered by Muse cells.¹³ The paracrine effects of Muse cells included the production of matrix metalloproteinase 2 and 9, which might suppress scar formation and/or fibrosis^{13, 26}; production of hepatocyte growth factor and VEGF, which might have led to neovascularization and vascular protection^{13, 27-29}; and reduction of apoptotic cardiomyocytes, which might have contributed to the reduced infarct size.¹³ In the present study, the number of TUNEL⁺ cardiomyocytes was significantly smaller in the S1PR2 agonist group than in the vehicle group (Fig. 4E), and the capillary density in the border area was significantly greater in the S1PR2 agonist group than in the vehicle group (Fig. 4F). Therefore, anti-apoptotic effects and neovascularization as well as differentiation of Muse cells into cardiac- and vascular-lineage cells might have contributed to the observed reduction in the infarct size and the improved LV function, similar to findings of a previous study in which exogenous Muse cells were intravenously infused.¹³ Besides the improved degree of recovery, the beneficial elements delivered by the increase in endogenous Muse cells enhanced by administration of the S1PR2 agonist did not differ largely from that following infusion of exogenous Muse cells. Thus, the outcome of more efficient mobilization of endogenous Muse cells appears to be comparable to that of the donor-derived Muse cell treatment.

The standard and most effective therapy for human AMI is reperfusion of the occluded coronary artery as soon as possible by percutaneous coronary intervention. In AMI patients for whom coronary reperfusion therapy by percutaneous coronary intervention is too late or has failed, cardiac regenerative therapy is required to reconstruct the infarcted cardiac tissue and to prevent LV remodeling and heart failure. Stem cell therapy using exogenous Muse cells is a promising regenerative therapy.¹³ As the present study shows, another approach may be to enhance the mobilization endogenous Muse cells. Therefore, the present study provides important information for the clinical application of an S1PR2 agonist to enhance the mobilization of endogenous Muse cells, leading to structural and functional recovery of the infarcted heart.

As clinical implications for treating AMI patients, S1PR2 agonist treatment is a simple, low-cost method of promoting an increase supply of Muse cells to the peripheral blood compared with the administration of exogenous Muse cells, which requires cell culture and expansion. Some limitations must be overcome, because the infarct size-reducing effect in this study (30.5% reduction) of the S1PR2 agonist treatment

was lesser than that produced by intravenous injection of exogenous Muse cell treatment, as reported previously (55.5% reduction)¹³. However, considering that there are few drugs that deliver reduction of infarct size and improve cardiac functions when administered after the onset of AMI³⁰, the S1PR2 agonist may be a hopeful drug to improve cardiac function and attenuate remodeling. Although many issues still need to be addressed, the development of a clinical grade S1PR2 agonist may provide a new strategy for treating AMI patients.

Declarations

Author contributions

Shingo Minatoguchi conducted the experiments, and acquired and analyzed the data. Yoshihisa Yamada, Noriko Endo, Shohei Wakao, Yoshihiro Kushida, Hiromitsu Kanamori, Atsushi Mikami, and Hiroyuki Okura conducted the experiments. Mari Dezawa wrote the manuscript. Shinya Minatoguchi designed and supervised the research studies and wrote the manuscript.

Acknowledgements

This study was supported by Grants-in-Aid from the Japan Agency for Medical Research and Development (AMED) and from Ministry of Education, Culture, Sports, Science, and Technology and JSPS KAKENHI Grant Number JP18K15843, Japan.

Conflict of interest:

Y. Yamada and Shinya Minatoguchi of Gifu University, and S. Wakao, Y. Kushida, and M. Dezawa of Tohoku University are parties to a joint research agreement with Life Science Institute, Inc (LSII; Tokyo, Japan), respectively. S. Wakao and M. Dezawa have a patent for Muse cells, and the isolation method thereof licensed to LSII. Shinya Minatoguchi and M. Dezawa have a patent of Muse cells treatment for acute myocardial infarction. The other authors report no conflicts.

Data availability:

The datasets used and/or analysed during the current study available from the corresponding author on reasonable request.

References

1. Pfeffer MA, Braunwald E. Ventricular remodeling after myocardial infarction. Experimental observations and clinical implications. *Circulation* **81**:1161–1172 (1990).
2. Aso S, Imamura H, Sekiguchi Y, Iwashita T, Hirano R, Ikeda U, Okamoto K. Incidence and mortality of acute myocardial infarction. A population-based study including patients with out-of-hospital cardiac arrest. *Int Heart J* **52**:197–202 (2011).

3. Yeh RW, Sidney S, Chandra M, Sorel M, Selby JV, Go AS. Population trends in the incidence and outcomes of acute myocardial infarction. *N Engl J Med* **362**:2155–2165 (2010).
4. Chew DS, Heikki H, Schmidt G, Kavanagh KM, Dommasch M, Bloch Thomsen PE, Sinnecker D, Raatikainen P, Exner DV. Change in left ventricular ejection fraction following first myocardial infarction and outcome. *JACC Clin Electrophysiol* **4**:672–682 (2018).
5. Bolognese L, Neskovic AN, Parodi G, Cerisano G, Buonamici P, Santoro GM, Antoniucci D. Left ventricular remodeling after primary coronary angioplasty: Patterns of left ventricular dilation and long-term prognostic implications. *Circulation* **106**:2351–2357(2002).
6. Kuroda Y, Kitada M, Wakao S, Nishikawa K, Tanimura Y, Makinoshima H, Goda M, Akashi H, Inutsuka A, Niwa A, Shigemoto T, Nabeshima Y, Nakahata T, Nabeshima Y, Fujiyoshi Y, Dezawa M. Unique multipotent cells in adult human mesenchymal cell populations. *Proc Natl Acad Sci U S A* **107**:8639–8643 (2010).
7. Wakao S, Kitada M, Kuroda Y, Shigemoto T, Matsuse D, Akashi H, Tanimura Y, Tsuchiyama K, Kikuchi T, Goda M, Nakahata T, Fujiyoshi Y, Dezawa M. Multilineage-differentiating stress-enduring (Muse) cells are a primary source of induced pluripotent stem cells in human fibroblasts. *Proc Natl Acad Sci U S A* **108**:9875–9880 (2011).
8. Tanaka T, Nishigaki K, Minatoguchi S, Nawa T, Yamada Y, Kanamori H, Mikami A, Ushikoshi H, Kawasaki M, Dezawa M, Minatoguchi S. Mobilized Muse cells after acute myocardial infarction predict cardiac function and remodeling in the chronic phase. *Circ J* **82**:561–571(2018).
9. Wakao S, Kushida Y, Dezawa M. Basic characteristics of Muse cells. *Adv Exp Med Biol* **1103**:13–41(2018).
10. Guo Y, Xue Y, Wang P, Cui Z, Cao J, Liu S, Yu Q, Zeng Q, Zhu D, Xie M, Zhang J, Li Z, Liu H, Zhong J, Chen J. Muse cell spheroids have therapeutic effect on corneal scarring wound in mice and tree shrews. *Sci Transl Med* **12** (562):eaaw1120 (2020).
11. Hori E, Hayakawa Y, Hayashi T, Hori S, Okamoto S, Shibata T, Kubo M, Horie Y, Sasahara M, Kuroda S. Mobilization of pluripotent multilineage-differentiating stress-enduring cells in ischemic stroke. *J Stroke Cerebrovasc Dis* **25**:1473–1481(2016).
12. Minatoguchi S, Ando T, Tanaka T, Yamada Y, Kanamori H, Kawasaki M, Nishigaki K, Minatoguchi S. Cardiac rehabilitation with dynamic exercise increases the number of Muse cells in the peripheral blood of patients with heart disease. *Circ Rep* **1**:17–19 (2018).
13. Yamada Y, Wakao S, Kushida Y, Minatoguchi S, Mikami A, Higashi K, Baba S, Shigemoto T, Kuroda Y, Kanamori H, Amin M, Kawasaki M, Nishigaki K, Taoka M, Isobe T, Muramatsu C, Dezawa M, Minatoguchi S. S1P-S1PR2 axis mediates homing of Muse cells into damaged heart for long-lasting tissue repair and functional recovery after acute myocardial infarction. *Circ Res* **122**:1069–1083 (2018).
14. Abe T, Aburakawa D, Niizuma K, Iwabuchi N, Kajitani T, Wakao S, Kushida Y, Dezawa M, Borlongan CV, Tominaga T. Intravenously transplanted human multilineage-differentiating stress-enduring cells afford brain repair in a mouse lacunar stroke model. *Stroke* **51**:601–611(2020).

15. Iseki M, Kushida Y, Wakao S, Akimoto T, Mizuma M, Motoi F, Asada R, Shimizu S, Unno M, Chazenbalk G, Dezawa M. Muse cells, nontumorigenic pluripotent-like stem cells, have liver regeneration capacity through specific homing and cell replacement in a mouse model of liver fibrosis. *Cell Transplant* **26**:821–840 (2017).
16. Uchida N, Kushida Y, Kitada M, Wakao S, Kumagai N, Kuroda Y, Kondo Y, Hirohara Y, Kure S, Chazenbalk G, Dezawa M. Beneficial effects of systemically administered human Muse cells in adriamycin nephropathy. *J Am Soc Nephrol* **28**:2946–2960 (2017).
17. Fujita Y, Komatsu M, Lee SE, Kushida Y, Nakayama-Nishimura C, Matsumura W, Takashima S, Shinkuma S, Nomura T, Masutomi N, Kawamura M, Dezawa M, Shimizu H. Intravenous injection of Muse cells as a potential therapeutic approach for epidermolysis bullosa. *J Invest Dermatol* **141**:198–202 e196 (2021).
18. Yamashita T, Kushida Y, Wakao S, Tadokoro K, Nomura E, Omote Y, Takemoto M, Hishikawa N, Ohta Y, Dezawa M, Abe K. Therapeutic benefit of Muse cells in a mouse model of amyotrophic lateral sclerosis. *Sci Rep* **10**:17102 (2020).
19. Noda T, Nishigaki K, Minatoguchi S. Safety and efficacy of human Muse cell-based product for acute myocardial infarction in a first-in-human trial. *Circ J* **84**:1189–1192(2020).
20. Fujita Y, Nohara T, Takashima S, Natsuga K, Adachi M, Yoshida K, Shinkuma S, Takeichi T, Nakamura H, Wada O, Akiyama M, Ishiko A, Shimizu H. Intravenous allogeneic multilineage-differentiating stress-enduring cells in adults with dystrophic epidermolysis bullosa: A phase 1/2 open-label study. *J Eur Acad Dermatol Venereol* **35**: e528-e531 (2021).
21. Tiper IV, East JE, Subrahmanyam PB, Webb TJ. Sphingosine 1-phosphate signaling impacts lymphocyte migration, inflammation and infection. *Pathog Dis* **74** (6):ftw063.(2016).
22. Adada M, Canals D, Hannun YA, Obeid LM, *FEBS Journal* **280**: 6354–6366 (2013)
23. Minatoguchi S, Takemura G, Chen XH, Wang N, Uno Y, Koda M, Arai M, Misao Y, Lu C, Suzuki K, Goto K, Komada A, Takahashi T, Kosai K, Fujiwara T, Fujiwara H. Acceleration of the healing process and myocardial regeneration may be important as a mechanism of improvement of cardiac function and remodeling by postinfarction granulocyte colony-stimulating factor treatment. *Circulation* **109**:2572–2580 (2004).
24. Chen XH, Minatoguchi S, Kosai K, Yuge K, Takahashi T, Arai M, Wang N, Misao Y, Lu C, Onogi H, Kobayashi H, Yasuda S, Ezaki M, Ushikoshi H, Takemura G, Fujiwara T, Fujiwara H. In vivo hepatocyte growth factor gene transfer reduces myocardial ischemia-reperfusion injury through its multiple actions. *J Card Fail* **13**:874–883 (2007).
25. Metzler B, Hammerer-Lercher A, Jehle J, Dictrich H, Pachinger O, Xu Q, Mair J. Plasmatroponin T closely correlates with infarct size in a mouse model of acute myocardial infarction. *Clin Chim Acta* **325**: 87–90 (2002).
26. Mias C, Lairez O, Trouche E, Roncalli J, Calise D, Seguelas MH, Ordener C, Piercecchi-Marti MD, Auge N, Salvayre AN, Bourin P, Parini A, Cussac D. Mesenchymal stem cells promote matrix

- metalloproteinase secretion by cardiac fibroblasts and reduce cardiac ventricular fibrosis after myocardial infarction. *Stem Cells* **27**:2734–2743 (2009).
27. Shono Y, Kushida Y, Wakao S, Kuroda Y, Unno M, Kamei T, Miyagi S, Dezawa M. Protection of liver sinusoids by intravenous administration of human Muse cells in a rat extra-small partial liver transplantation model. *Am J Transplant* **21**: 2025–2039 (2021).
28. Isner JM, Losordo DW. Therapeutic angiogenesis for heart failure. *Nat Med* **5**:491–492 (1999).
29. Asahara T, Takahashi T, Masuda H, Kalka C, Chen D, Iwaguro H, Inai Y, Silver M, Isner JM. VEGF contributes to postnatal neovascularization by mobilizing bone marrow-derived endothelial progenitor cells. *EMBO J* **18**:3964–3972 (1999).
30. Minatoguchi S. Cardioprotection against acute myocardial infarction. Springer Nature Singapore Pte Ltd, <https://doi.org/10.1007/978-981-15-0167-8> (2019).

Figures

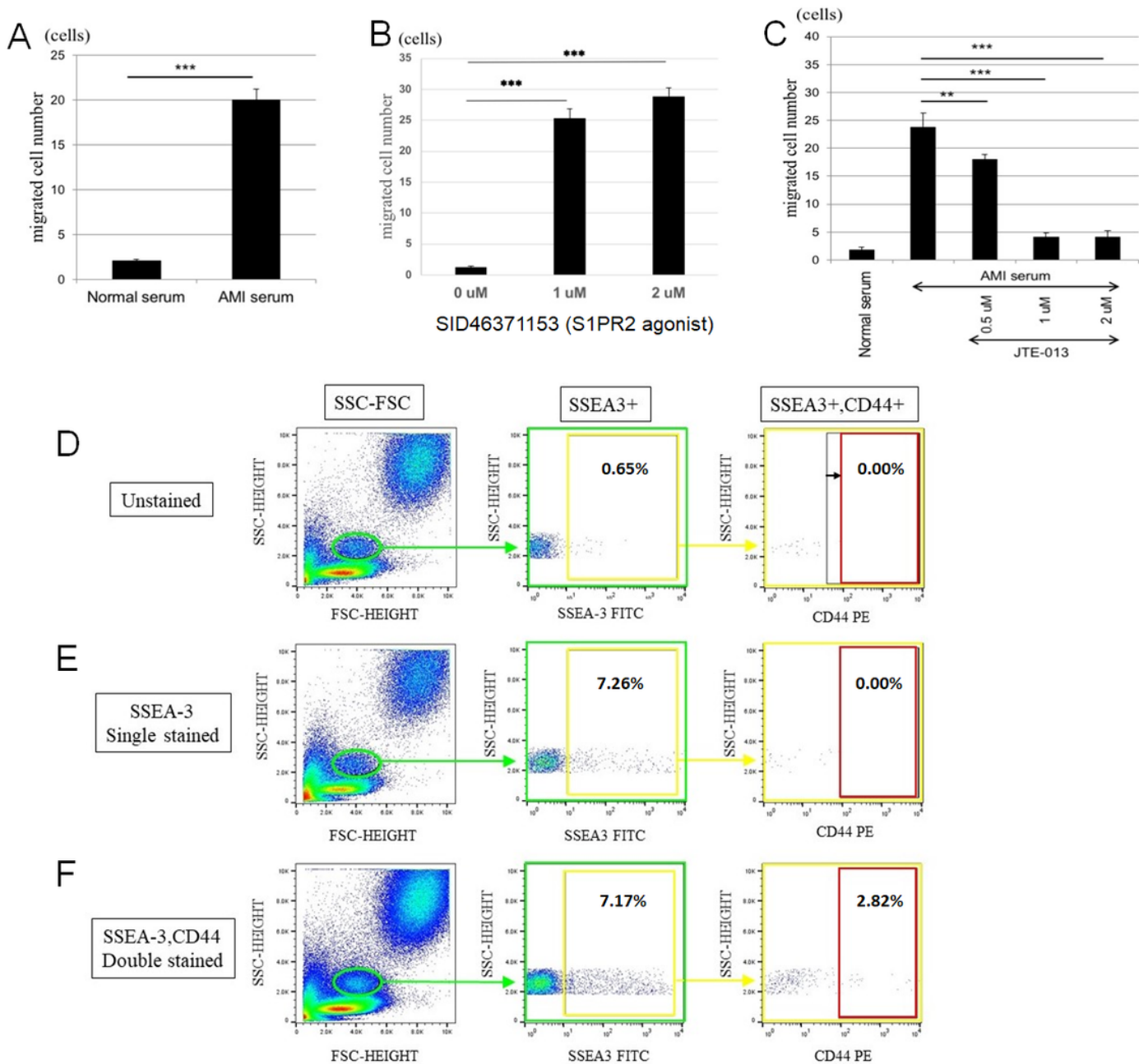


Figure 1

In vitro analysis of Muse cell migration and cardiac-lineage differentiation

A-C: Migration assay of Muse cells. Migration of rabbit Muse cells toward rabbit AMI serum (A), S1PR2 agonist SID46371153 (B). Suppression of rabbit Muse cell migration toward rabbit AMI serum by the S1PR2 antagonist JTE-013 (C). **D-F:** Scattergram of the fluorescence-minus-one control method. (D) Unstained peripheral blood from rabbit in the sham group. Green gated oval: monocyte area, Yellow square: SSEA-3+ area (non-specific false-positive cells), Black square: approximate temporary SSEA3/CD44 double-positive area, Red square: SSEA-3 and CD44 double-positive area compared with the results of the single stains (E). Because this is an unstained sample, SSEA-3/CD44 double-positive cells

are considered to be in the red square area. (E) SSEA-3 single-stained cells in peripheral blood from the sham group. (F) SSEA-3/CD44 double-stained cells in the peripheral blood from the sham group.

A: n=5 in each bar, p<0.001, unpaired Student's t-test, **B-C:** n=5 in each bar, p<0.01 and P<0.001, 1-way analysis of variance followed by multiple comparisons with the Dunnett method,

G-I: n=5 in each bar of day 1, 7, 10, 17, 24 and 31, p<0.05, 1-way analysis of variance followed by multiple comparisons with the Dunnett method,

*: p<0.05, **: p<0.01, ***: p<0.001

Fig.2

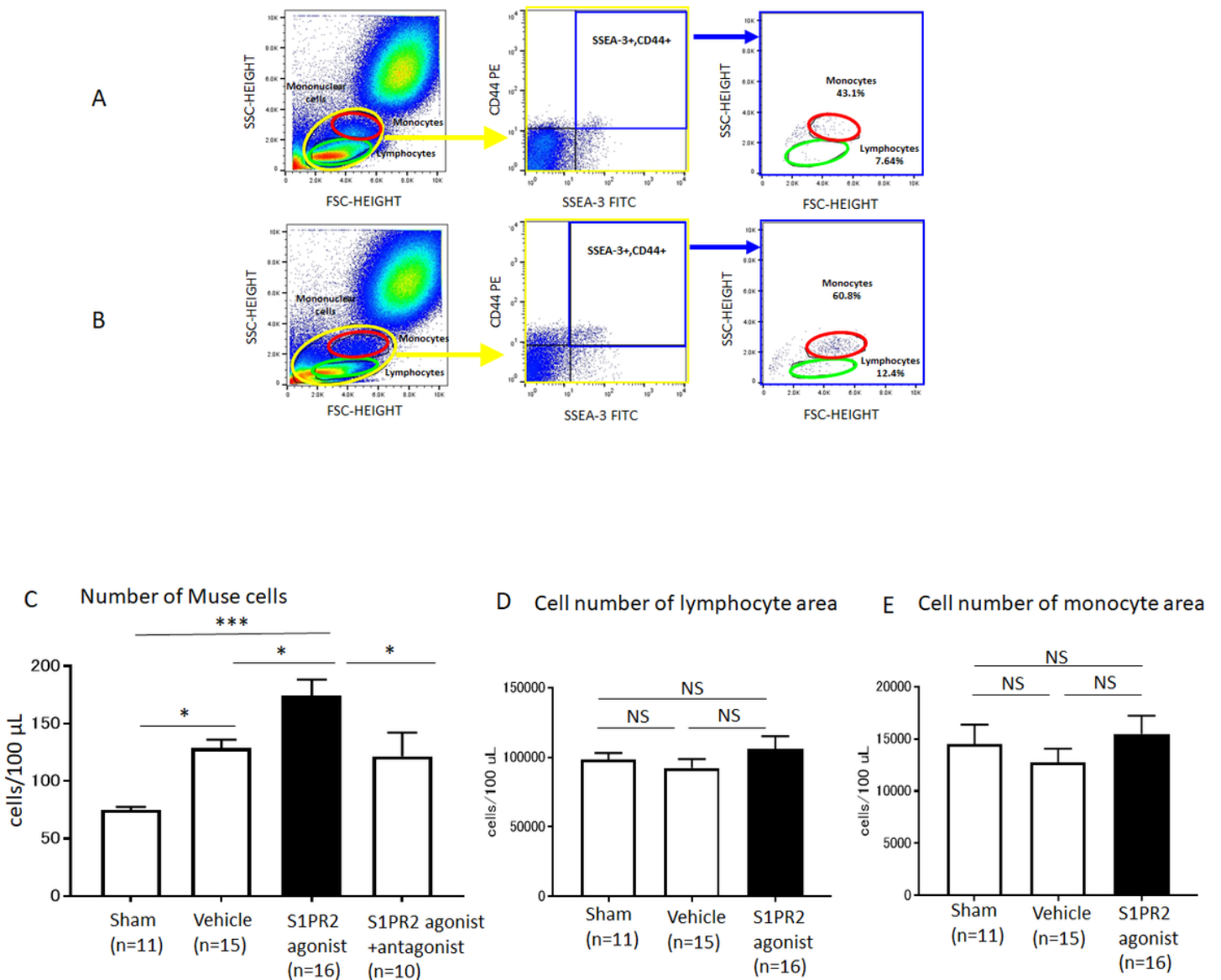


Figure 2

Flow cytometry of the rabbit peripheral blood after S1PR2 agonist treatment.

A,B: Typical images of flow cytometry in the vehicle and S1PR2 agonist groups. We gated the mononuclear cell area, and monocyte and lymphocyte areas (forward scatter [FSC] and side scatter [SSC] of the flow cytometer were focused on mononuclear cells; all cells). Distribution of SSEA-3/CD44 double-positive Muse cells in the mononuclear cell area, monocyte area, and lymphocyte area within the gated area (Muse cells). Percent of Muse cells in the monocyte and lymphocyte areas is indicated as the percent of Muse cells to that in the total mononuclear cell area. Number of Muse cells in the monocyte area was defined as the number of Muse cells in the peripheral blood because the majority of Muse cells were detected in the monocyte area and fewer Muse cells were detected in the lymphocyte area. Furthermore, clear gating of the lymphocyte area is sometimes difficult due to debris located close to the lymphocyte area. **C-E:** Muse cell number in the peripheral blood in the 4 groups. C: Number of SSEA-3/CD44-double-positive Muse cells in the peripheral blood of the sham (n=11), vehicle (n=15), S1PR2 agonist (n=16), and S1PR2 agonist+antagonist (n=10) groups. *: $P < 0.05$, ***: $p < 0.001$, 1-way analysis of variance followed by multiple comparisons with the Tukey method, D: Number of whole cells in the lymphocyte area in the sham (n=11), vehicle (n=15), and S1PR2 agonist (n=16) groups. No difference was detected among the 3 groups. 1-way analysis of variance followed by multiple comparisons with the Tukey method, E: Number of whole cells in the monocyte area in the sham (n=11), vehicle (n=15), and S1PR2 agonist (n=16) groups. No difference was detected among the 3 groups. 1-way analysis of variance followed by multiple comparisons with the Tukey method, NS; not significant.

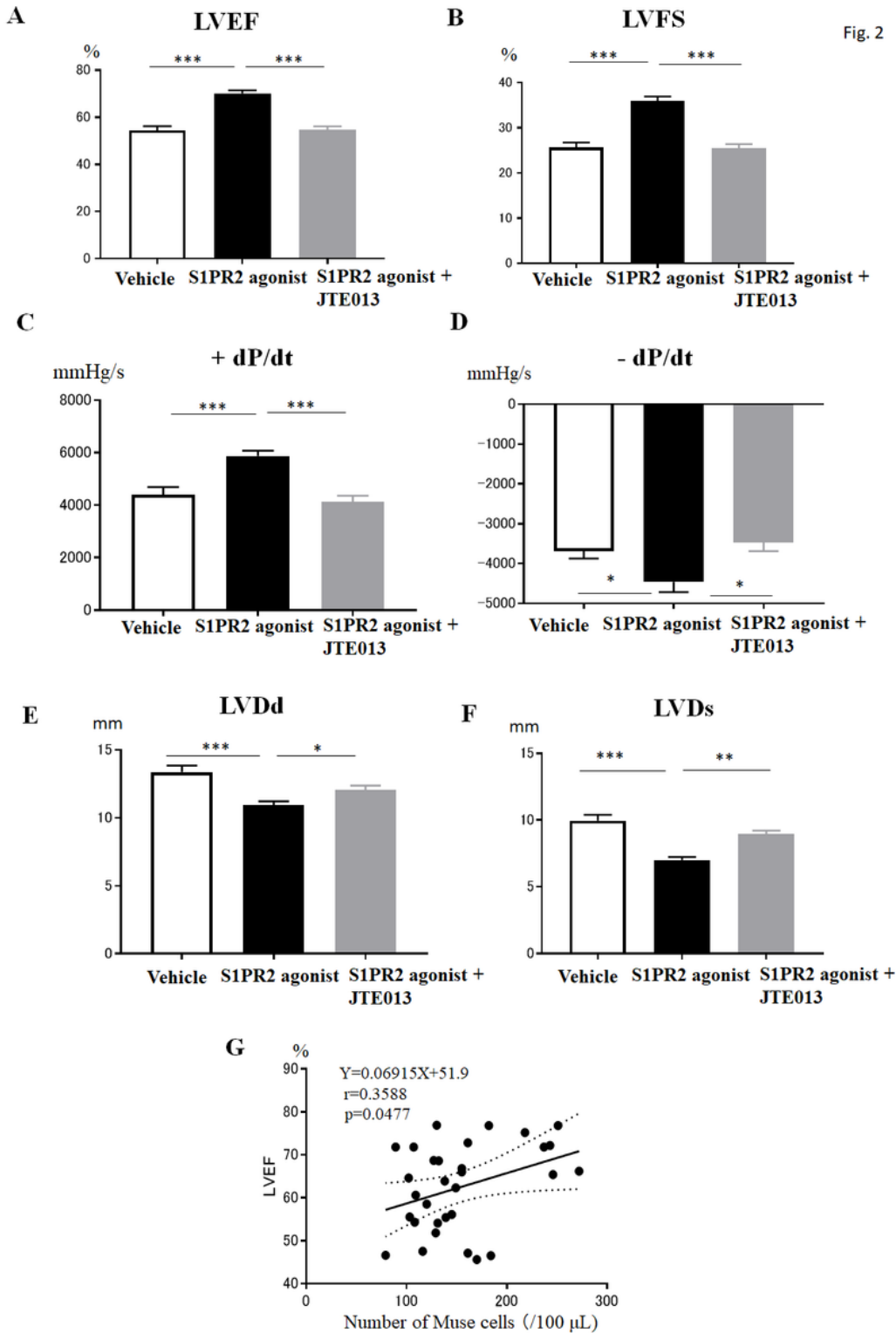


Figure 3

Physiologic analysis

LV ejection fraction (LVEF)(**A**), LV fractional shortening (LVFS)(**B**), LV end-diastolic dimension (LVDd)(**E**), and LV end-systolic dimension (LVDs)(**F**) were assessed by echocardiography in the vehicle, S1PR2 agonist, and S1PR2 agonist+antagonist groups. The +dP/dt (**C**) and -dP/dt (**D**) were assessed using a

Millar catheter. **G:** Relationship between the number of Muse cells in the peripheral blood after AMI and LV function.

A-F: Vehicle (n=15), S1PR2 agonist group (n=16), S1PR2 agonist+antagonist group (n=10),

*: p<0.05, **: p<0.01, ***: p<0.001: 1-way analysis of variance followed by multiple comparisons with the Tukey method, **G:** n=31(vehicle and S1PR2 agonist groups), p<0.05, linear regression analysis

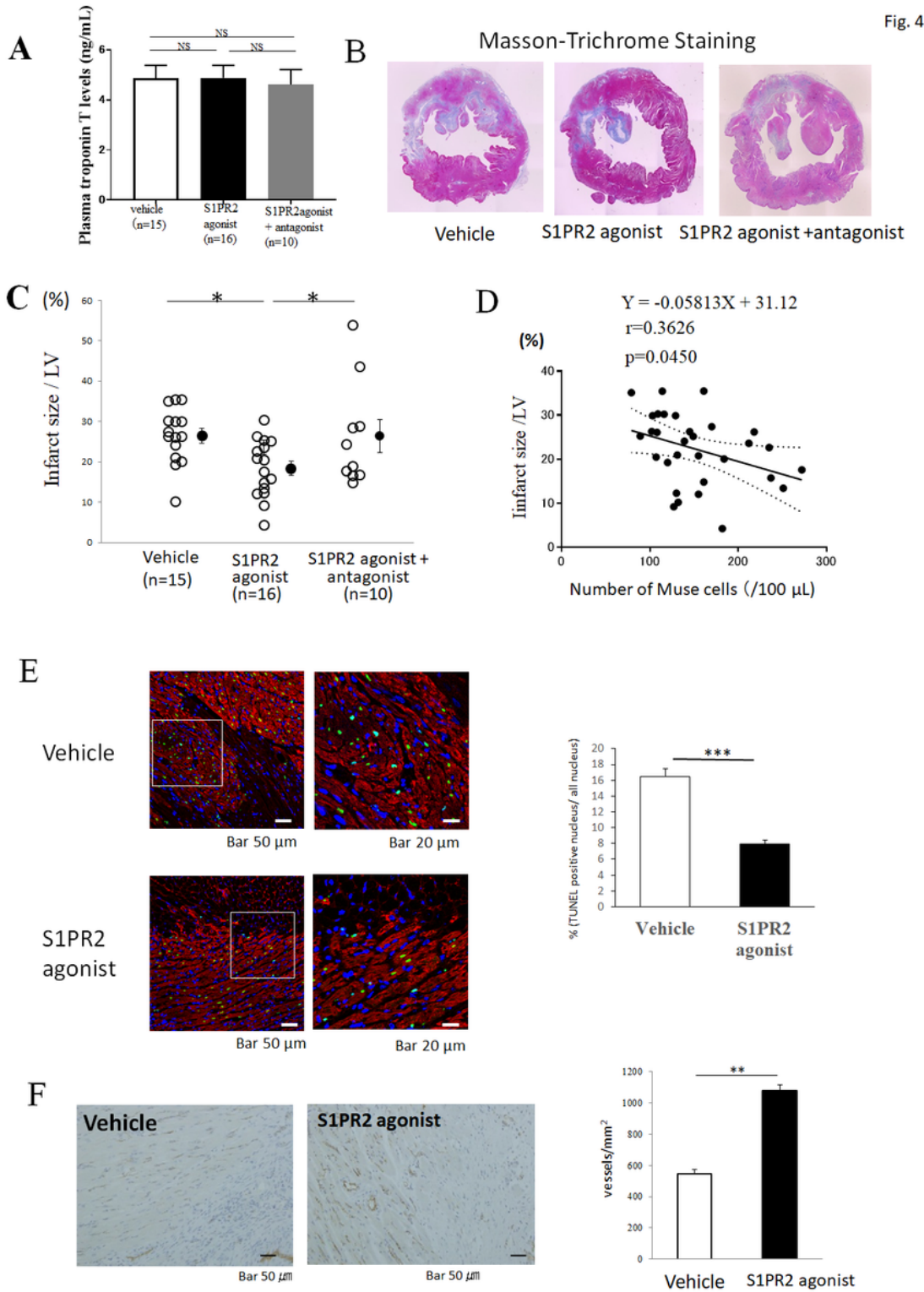


Figure 4

Myocardial infarct size and histologic analysis.

A: Plasma troponin T levels 24 h after AMI. Vehicle (n=15), S1PR2 agonist group (n=16), S1PR2 agonist+antagonist group (n=10). **B:** Typical figures of transverse LV sections at the papillary muscle level stained by Masson-trichrome at 2 weeks. **C:** The infarct size as a percent of the total LV area among the 3 groups at 2 weeks. Vehicle (n=15), S1PR2 agonist group (n=16), S1PR2 agonist+antagonist group (n=10), $p < 0.05$, 1-way analysis of variance followed by multiple comparisons with the Tukey method. **D:** Relation between the number of Muse cells in the peripheral blood after AMI and the infarct size. $n = 31$ (vehicle and S1PR2 agonist groups), $p < 0.05$, linear regression analysis. **E:** TUNEL-positive cardiomyocytes in the vehicle (n=5) and S1PR2 agonist (n=5) groups at 3 days. Red signal: cardiomyocytes stained by myoglobin, Green signal: apoptotic cells detected by TUNEL, Blue signal: nucleus stained with Hoechst 33342. 20 observations in each, $p < 0.001$, unpaired Student's t-test. **F:** CD31-positive cells at the border area in the vehicle (n=5) and S1PR2 agonist (n=5) groups at 2 weeks. 20 observations in each, $p < 0.01$, unpaired Student's t-test

*: $p < 0.05$, **: $p < 0.01$, ***: $p < 0.001$

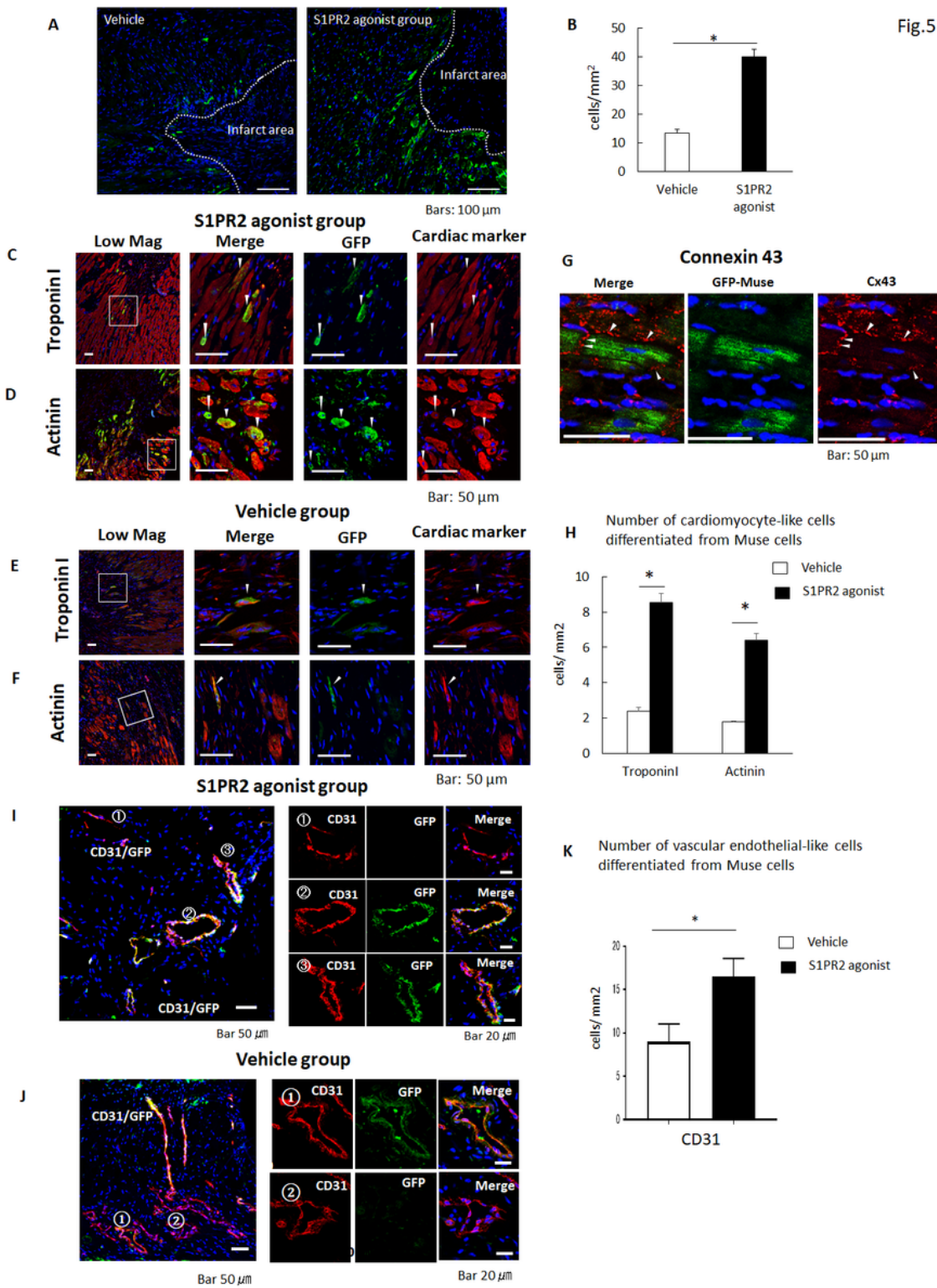


Figure 5

Cardiac marker expression in the vehicle and S1PR2 agonist groups at 14 days after AMI.

A: GFP-positive Muse cells engrafted in the infarct and border areas of the myocardium in the vehicle (n=5) and S1PR2 agonist (n=5) groups. **B:** Number of GFP-positive Muse cells per mm^2 engrafted in the infarct and border areas of the myocardium in the vehicle and S1PR2 agonist groups. (20 observations in

each, $p < 0.05$, unpaired student's t-test) **C-F**: GFP-positive Muse cells expressed troponin I and sarcomeric α -actinin, markers of cardiomyocytes in the S1PR2 agonist (C, D) and vehicle (E, F) groups. **G**: GFP-positive Muse cells expressed connexin 43, a marker of gap junction. **H**: Number of GFP- and troponin I-double-positive cells, and GFP- and sarcomeric α -actinin-double-positive cells in the vehicle and S1PR2 agonist groups. (20 observations in each, $p < 0.05$, unpaired student's t-test) **I, J**: GFP-positive Muse cells expressed CD31, a marker of vascular endothelial cells, in the S1PR2 agonist (I) and vehicle (J) groups. (1) in I is an endogenous vessel, while (2) and (3) are vessels incorporated with GFP+ Muse cells. Similarly, (1) is vessel incorporated with GFP+ Muse cells and (2) is an endogenous vessel. **K**: Number of GFP- and CD31 double-positive cells in the vehicle and S1PR2 agonist groups. (20 observations in each, $p < 0.05$, unpaired student's t-test) *: $p < 0.05$.

Supplementary Files

This is a list of supplementary files associated with this preprint. Click to download.

- [SupplementalOnlinedata.docx](#)